Published in final edited form as:
J Struct Biol. 2010 May ; 170(2): 334–343. doi:10.1016/j.jsb.2009.11.013.

ALTERED MYOFILAMENT FUNCTION DEPRESSES FORCE GENERATION IN PATIENTS WITH NEBULIN-BASED NEMALINE MYOPATHY (NEM2)

Coen A.C. Ottenheijm[1,2], **Pleuni Hooijman**[1], **Elizabeth T. DeChene**[3], **Ger J. Stienen**[1], **Alan H. Beggs**[3], and **Henk Granzier**[2]

[1] Laboratory for Physiology, Institute for Cardiovascular Research, VU University Medical Center, Amsterdam 1081 BT, the Netherlands [2] Dept of Physiology, University of Arizona, Tucson, AZ 85724, USA [3] Division of Genetics and Program in Genomics, The Manton Center for Orphan Disease Research, Children's Hospital Boston, Harvard Medical School, Boston, MA 02115, USA

Abstract

Nemaline myopathy (NM), the most common non-dystrophic congenital myopathy, is clinically characterized by muscle weakness. However, the mechanisms underlying this weakness are poorly understood. Here, we studied the contractile phenotype of skeletal muscle from NM patients with nebulin mutations (NEM2). SDS-PAGE and Western blotting studies revealed markedly reduced nebulin protein levels in muscle from NM patients, whereas levels of other thin filament-based proteins were not significantly altered. Muscle mechanics studies indicated significantly reduced calcium sensitivity of force generation in NM muscle fibers compared to control fibers. In addition, we found slower rate constant of force redevelopment, as well as increased tension cost, in NM compared to control fibers, indicating that in NM muscle the rate of cross bridge attachment is reduced, whereas the rate of cross bridge detachment is increased. The resulting reduced fraction of force generating cross bridges is expected to greatly impair the force generating capacity of muscle from NM patients. Thus, the present study provides important novel insights into the pathogenesis of muscle weakness in nebulin-based NM.

Keywords

nemaline myopathy; nebulin; muscle weakness; crossbridge cycling; thin filament length

INTRODUCTION

Nemaline myopathy (NM) is the most common non-dystrophic congenital myopathy, with an estimated incidence of ~1 per 50,000 live births [1]. NM is characterized at the muscle's ultrastructural level by the presence of rod-shaped structures (nemaline rods) in affected muscle fibers [2]. Clinically, the most prominent feature of NM is generalized muscle

Corresponding author: Henk Granzier, Dept of Physiology, University of Arizona, PO Box 245217, Tucson, AZ 85724, Voice: 520-626-3641, Fax: 520-626-7600, granzier@email.arizona.edu.

weakness that greatly affects the daily-life activities, and the quality of life of these patients [3].

NM is a genetically heterogeneous disorder of the skeletal muscle thin filament caused by mutations in any one of at least six different genes, all encoding thin filament proteins of the sarcomere: *ACTA1* (actin), *TPM3* and *TPM2* (α and β tropomyosin), *TNNT1* (troponinT), *CFL2* (cofilin-2), and *NEB* (nebulin), for a review see Sanoudou and Beggs [4]. Despite detailed knowledge of the underlying genetic basis for NM in many patients, the mechanisms underlying muscle weakness in NM patients are poorly understood.

Mutations in the nebulin gene are the most common cause of NM (patients referred to as NEM2), accounting for ~50% of all NM cases [5]. Nebulin is a giant protein (MW ~800 kDa) expressed at high levels in skeletal muscle. A single nebulin molecule spans the thin filament with its C-terminus anchored at the Z-disk and its N-terminal region directed towards the thin filament pointed end [6]. Previous studies [7;8] revealed that nebulin-deficient murine muscle fibers have thin filaments that vary in length [7] and that are on average shorter than in wildtype muscle [7;8], supporting the notion that nebulin is important in establishing thin filament length. Thin filament length is an important aspect of muscle function as the extent of overlap between thick and thin filaments determines the sarcomere's force generating capacity: short thin filaments reduce overlap and impair force generation. In accordance with a role for nebulin in establishing thin filament length, we have shown that similar to the nebulin knockout (KO) mouse model, human NM patients with nebulin-deficiency also have shorter and non-uniform thin filament lengths, which can partly account for the observed muscle weakness in nebulin-based NM [9].

Recent studies on nebulin knockout mouse models suggest that nebulin's role in muscle function extends beyond a purely structural one, and involves a role in the regulation of cross bridge cycling kinetics and thin filament activation. It was found that nebulin increases the fraction of force generating cross-bridges that is available in the overlap zone [10;11] and enhances the force response to submaximal calcium concentrations [10]. Thus, in the nebulin KO mouse model reduced active tension and calcium sensitivity of force generation has been reported. Here we tested whether similar characteristics are present in muscle from NM patients with nebulin gene mutations. We found a reduced rate of force development as well as increased tension cost in nebulin-deficient muscle fibers from NM patients. Moreover, force generation in response to submaximal calcium concentrations was significantly decreased. These findings suggest altered cross bridge cycling kinetics and thin filament activation in nebulin-deficient fibers from NM patients, and provide a novel mechanism for muscle weakness in nebulin-based NM.

METHODS

Muscle biopsies from nemaline myopathy patients

Skeletal muscle specimens, remaining from diagnostic procedures or obtained during clinically indicated surgical procedures, were collected from four nemaline myopathy patients following informed consent supervised by the Children's Hospital Boston institutional review board, and from four unaffected control subjects, and stored frozen and unfixed at −80°C until use (Table 1). All four NM patients had mutations in the nebulin gene, including three patients who were homozygous for the previously described deletion of exon 55 [12] and one patient with a heterozygous single base deletion (p.Ser1908AlafsX8) resulting in a premature stop codon and an unidentified second mutation. Two of the three patients with the exon 55 deletion (biopsies T11 and T12) were included in the original report of this mutation by Anderson et al. [12] and all three patients

with this deletion (biopsies T11, T12, and T124) were previously described by Lehtokari et al. [13].

Gel electrophoresis and Western blotting

For nebulin expression, muscle samples were homogenized and analyzed on 2.6–7% SDS-acrylamide gels [9]. To prevent protein degradation, all buffers contained protease inhibitors (phenylmethylsulfonyl fluoride (PMSF), 0.5mM; leupeptin, 0.04mM; E64, 0.01mM). Gels were scanned and analyzed with One-D scan EX (Scanalytics Inc., Rockville, MD, USA) software. The integrated optical density of nebulin, myosin heavy chain (MHC), and actin was determined. For Western blot analysis of the thin filament-based regulatory proteins, 3.75–12% acrylamide gels were used. For troponin expression patterns, Western blotting was performed using fast-skeletal and slow-skeletal specific antibodies (ss-TnI: cs-20645; fs-TnI: sc-8120; ssTnT: sc-28269; fs-TnT sc-8123), and a troponinC antibody (sc-8117) that recognizes both slow- and fast-skeletal troponinC (Santa Cruz Biotechnology Inc, USA). For tropomyosin expression, Western blotting was performed using an antibody directed against both α- and β-tropomyosin (CH1, Hybridoma Bank, University of Iowa). Secondary antibodies conjugated with fluorescent dyes with infrared excitation spectra were used for detection. One or two-color infrared western blots were scanned (Odyssey Infrared Imaging System, Li-Cor Biosciences, NE. USA) and the images analyzed with One-D scan EX. For myosin heavy chain isoform composition, skeletal muscles were denatured by boiling for 2 min. The stacking gel contained a 4% acrylamide concentration (pH 6.7), and the separating gel contained 7% acrylamide (pH 8.7) with 30% glycerol (v/v). The gels were run for 24h at 15°C and a constant voltage of 275V. Finally, the gels were silver-stained, scanned, and analyzed with One-D scan EX software.

Immunofluorescence confocal scanning laser microscopy

Small strips were dissected from the biopsies and skinned overnight at ~4°C in relaxing solution (in mM; 20 BES, 10 EGTA, 6.56 $MgCl_2$, 5.88 NaATP, 1 DTT, 46.35 K-propionate, 15 creatine phosphate, pH 7.0 at 20°C) containing 1% (v/v) Triton X-100. To prevent protein degradation, the solutions contained protease inhibitors (phenylmethylsulfonyl fluoride (PMSF), 0.5mM; Leupeptin, 0.04mM; E64, 0.01mM). Immuno-labeling and confocal scanning laser microscopy was performed essentially as described previously [9], using Alexa Fluor 488 conjugated phalloidin (A12379, Invitrogen). Images were produced using a Bio-Rad MRC 1024 confocal laser scanning microscope using the LaserSHARP 2000 software package (Hercules, CA, USA). From the acquired images, thin filament lengths were determined using ImageJ software (National Institutes of Health).

Muscle mechanics

Small strips dissected from muscle biopsies were skinned overnight (as described above). The skinning procedure renders the membranous structures in the muscle fibres permeable, which enables activation of the myofilaments with exogenous Ca^{2+}. Preparations were washed thoroughly with relaxing solution and stored in 50% glycerol/relaxing solution at −20°C for up to ~8 weeks. Small muscle bundles (diameter ~0.07 mm) were dissected from the skinned strips, and were mounted between a displacement generator and a force transducer element (AE 801, SensoNor, Norway) using aluminum T-clips. Sarcomere length (SL) was set using a He-Ne laser diffraction system. Mechanical experiments on contracting muscle were carried out at an SL of ~2.5 μm for control muscle, and at just over slack length for NM muscle: a length selected for the following reason. By constructing force-SL relations we [9] previously showed that at an SL of 2.5 μm human muscle fibers from controls produced maximal force, whereas nebulin-deficient muscle fibers from NM patients produced maximal force just over slack length, due to their shorter thin filaments [9]. Thus, by performing our mechanical studies on NM muscle set just over slack length, we aimed to

minimize force differences due to shorter thin filament lengths. Fiber width and diameter were measured at three points along the fiber and the cross-sectional area was determined assuming an elliptical cross-section. Three different bathing solutions were used during the experimental protocols: a relaxing solution, a pre-activating solution with low EGTA concentration, and an activating solution. The composition of these solutions was as described previously [14].

Force-pCa relations—To determine the force-pCa relation (pCa = −log of molar free Ca^{2+} concentration), skinned muscle fiber bundles were sequentially bathed in solutions with pCa values ranging from 4.5 to 9.0 and the steady-state force was measured. Measured force values were normalized to the maximal force obtained at pCa 4.5. The obtained force-pCa data were fit to the Hill equation, providing pCa_{50} (pCa giving 50% maximal active tension) and the Hill coefficient, n_H, an index of myofilament cooperativity.

K_{tr} measurements—To measure the rate of tension redevelopment (Ktr), we used the large slack/release approach [15], to disengage force generating cross bridges from the thin filaments, which were isometrically activated. Fast activation of the fiber was achieved by transferring the skinned muscle fibers from the pre-activation solution containing a low concentration of EGTA (pCa 9.0) to a pCa 4.5 activating solution. Once the steady-state was reached, a slack equivalent to 10% of the muscle length was rapidly induced at one end of the muscle using the motor. This was followed immediately by an unloaded shortening lasting 30 msec. The remaining bound cross-bridges were mechanically detached by rapidly (1 msec) restretching the muscle fiber to its original length, after which tension redevelops. The rate constant of monoexponential tension redevelopment (K_{tr}) was determined by fitting the rise of tension to the following equation: $F=F_{ss}(1-e^{-Ktr.t})$, where F is force at time t and k_{tr} is the rate constant of tension redevelopment.

Simultaneous force-ATPase measurement—We used the system described by Stienen et al [14]. To measure the ATPase activity, a near UV light was projected through the quartz window of the bath (30 μl volume and temperature controlled at 20°C) and detected at 340 nm. The maximum activation buffer (pCa 4.5) contained 10 mM phosphoenol pyruvate, with 4 mg ml^{-1} pyruvate kinase (500 U mg^{-1}), 0.24 mg ml^{-1} lactate dehydrogenase (870 U mg^{-1}) and 20 μM diadenosine-5′ pentaphosphate (A_2P_5). For efficient mixing, the solution in the bath was continuously stirred by means of motor-driven vibration of a membrane positioned at the base of the bath. ATPase activity of the skinned fiber bundles was measured as follows: ATP regeneration from ADP is coupled to the breakdown of phosphoenol pyruvate to pyruvate and ATP catalyzed by pyruvate kinase, which is linked to the synthesis of lactate catalyzed by lactate dehydrogenase. The breakdown of NADH, which is proportional to the amount of ATP consumed, is measured on-line by UV absorbance at 340 nm. The ratio of light intensity at 340 nm (sensitive to NADH concentration), and the light intensity at 410 nm (reference signal), is obtained by means of an analog divider. After each recording, the UV absorbance signal of NADH was calibrated by multiple rapid injections of 0.25 nmol of ADP (0.025 μl of 10 mM ADP) into the bathing solution, with a stepper motor-controlled injector. The slope of the [ATP] vs. time trace during steady-state tension development of a calcium-induced contraction (see figure 5A) was determined from a linear fit and the value divided by the fiber volume (in mm^3) to determine the fiber's ATPase rate. ATPase rates were corrected for the basal ATPase measured in relaxing solution. The ATPase rate was divided by tension (force/CSA) to determine the tension cost.

RESULTS

Nebulin protein levels in NEM2 patients and controls

We studied skeletal muscle of four NM patients with nebulin mutations and four control subjects with no history of skeletal muscle disease (for control subject and patient characteristics see Table 1). Three of the patients had homozygous deletions of exon 55 of the nebulin gene and the fourth patient had a heterozygous single base pair deletion resulting in a premature stop codon (p.Ser1908AlafxX8) and a second unidentified mutation.

To study protein levels of nebulin, as well as the levels of other sarcomeric proteins, we used SDS-PAGE and Western blotting techniques on skeletal muscle fibers from NEM2 patients and control subjects. As shown in figure 2A, control muscle shows a clear nebulin band at ~800 kDa, with an expression level of 0.070 ± 0.001 (nebulin/MHC ratio). SDS-PAGE showed that nebulin in NEM2 patients has a mobility that is indistinguishable from that of controls. Importantly, gel analysis indicated significantly reduced nebulin levels relative to MHC in NM muscle (NM: 21 ± 13% of controls, figure 2A, middle panel). The actin/MHC ratio was significantly reduced as well, although to a lesser extent when compared to the nebulin/MHC ratio (NM: 78 ± 3% of controls, figure 2A, right panel).

To test for stoichiometric changes in other components of the thin filament we studied the thin filament regulatory proteins TnI, TnT, TnC and tropomyosin (Tm) and included in the analysis slow and fast skeletal isoforms and both α- and β-Tm. Figure 2B indicates that the total expression level of TnI, TnT, and TnC, normalized to actin, were on average reduced in NM compared to control muscle, although this reduction was not found to be significant. Total tropomyosin was higher in NM than in control muscle (figure 2B), with no difference in the relative expression of α- and β-Tm (0.41 ± 0.03 vs. 0.51 ± 0.04, NM and control respectively). Analysis of the slow and fast isoforms of the troponins revealed that the NM patients express mainly slow skeletal (ss) isoforms, whereas controls express both slow and fast skeletal (fs) isoforms (ss/fs, TnC: 4.5 ± 1.2 vs. 0.5 ± 0.2; TnI: 4.6 ± 1.7 vs. 0.09 ± 0.01; TnT: 5.3 ± 2.0 vs. 0.4 ± 0.1, NM vs. control respectively, for typical WB result see figure 2B).

As the contractile performance of skeletal muscle fibers might depend on the fibers' MHC isoform composition, we used specialized SDS-PAGE to study MHC isoform expression in NM and control muscle. As shown in figure 2C, control muscle expressed a mixture of MHC I, 2A and 2X isoforms (49 ± 3%, 33 ± 3%, and 18 ± 0.4%, respectively). In contrast, muscle from the four NM patients contained only MHC type I, with one patient expressing a minor band (~30% of total MHC) corresponding to MHC 2A, see figure 2C.

In summary, muscle of NM patients had greatly reduced nebulin protein levels relative to MHC, whereas the expression level of actin was only slightly reduced. Nebulin protein levels, relative to actin, were reduced to a larger extent than the relative levels of the other thin-filament based proteins troponin and tropomyosin, which showed no or only slightly reduced expression. Furthermore, consistent with pathological data on the biopsies demonstrating a characteristic fiber type 1 predominance (Table 1), the muscle biopsies of the NM patients mainly contained MHC type slow as well as slow Tn isoforms.

Muscle structure analysis by confocal microscopy

To study the effect of reduced nebulin levels on muscle structure and thin filament length we used immunofluorescence confocal scanning laser microscopy with fluorescently labeled phalloidin (which binds filamentous actin with high affinity) on NM and control muscle. Both control and NM myofibrils showed the expected striated labelling patterns, although the labelling appeared more variable and more diffuse in NM myofibrils. We also found

dense actin accumulations in the NM muscle fiber (figure 3A), which most likely indicate nemaline rods. Importantly, controls showed broad actin labeling with uniform density (except for the Z-disk area where actin filaments overlap), whereas in NM myofibrils the labelling was narrower with decreasing intensity from the Z-disk towards the middle of the sarcomere (figure 3A). Densitometric analysis revealed that the width at half-maximal intensity was significantly reduced in NM compared to control myofibrils (figure 3B&C). Thus, these studies suggest shorter and non-uniform thin filament lengths in NM myofibrils.

Muscle fiber mechanics

As NM muscle expressed mainly MHC type I (figure 2C), and considering that a muscle fiber's contractile properties can depend on MHC isoform composition, the contractile data from NM muscle preparations were compared to those from control fibers expressing solely slow MHC. We found that the maximal Ca^{2+}-activated active tension (tension at pCa 4.5) was significantly reduced from 71 ± 8 mN/mm^2 in control to 5 ± 1 mN/mm^2 in the NM muscle fibers. We also measured active force at a range of calcium levels and expressed force relative to the maximal force. An example of active force development of a NM muscle preparation in response to incremental calcium is shown in figure 4A. The obtained force-pCa relations were shifted to the right in NM muscle fibers (figure 4B) with a pCa_{50} value of 5.67 ± 0.08 for control muscle fibers and 5.28 ± 0.07 for NM muscle fibers. NM muscle fibers also had on average a reduced Hill coefficient (n_H), a measure of the cooperativity of myofilament activation, but this difference was not statistically significant (figure 4B).

The tension cost was determined simultaneously by measurement of the breakdown of NADH and force during contraction, with NADH levels enzymatically coupled to ATP utilization (see Methods). An example of a maximally-activated NM muscle preparation with [NADH] falling linearly during the tension plateau is shown in figure 5A. The slope of the [NADH] vs. time curve was normalized by the fiber volume to obtain ATP consumption rates that can be compared for differently sized muscle preparations. By normalizing ATP consumption rates to the tension generated and fiber volume, the tension cost can be determined. As shown in figure 5B, the tension cost was significantly higher in NM muscle compared to control muscle (8.5 ± 0.8 vs. 3.0 ± 0.2 pmol/mN/mm/s, NM vs. control respectively).

We also measured the rate of tension redevelopment (K_{tr}). Muscle preparations were first isometrically activated at pCa 4.5 and when a steady tension was reached, crossbridges were disengaged by performing a quick release, a brief period of unloaded shortening, and then a rapid restretch to the original length. Following restretch, tension rebuilds with a time course that can be fit to a monoexponential with rate constant K_{tr}. Figure 6A illustrates a K_{tr} measurement on an NM and control muscle preparation, revealing that tension recovers slower in the NM than in the control muscle preparation. The averaged results from different fibers are shown in figure 6B. K_{tr} is significantly lower in NM fibers compared to control fibers (1.5 ± 0.2 vs. 2.2 ± 0.2 s^{-1}).

DISCUSSION

Although mutations in six different genes have been implicated in NM, mutations in the nebulin gene are the most common cause of NM [5]. Recent work indicated that in the absence of nebulin in murine muscle, cross bridge cycling kinetics are altered to reduce force production [10;11], and myofilament calcium sensitivity is reduced [10]. Here, we have studied NEM2 patients who have NM caused by nebulin gene mutations, resulting in severely reduced levels of nebulin protein compared to control muscles. Our findings indicate that in these nebulin-deficient muscle fibers from NM patients, the cross-bridge

attachment rate is slower and the cross-bridge detachment rate is faster. The resulting reduction in the number of force generating cross bridges in muscle fibers from these patients is expected to impair the force generating capacity of muscle. Furthermore, the force response to submaximal calcium concentrations was blunted in nebulin-deficient muscle fibers from NM patients, indicating reduced myofilament calcium sensitivity.

Sarcomeric protein levels in patients with NM

Nebulin is encoded by a single gene containing 183 exons in humans [16]. About 97% of these exons are 100–120 bp in length and code for a highly modular structure, the so-called SDXXYK-repeats (see figure 1). A total of 185 SDXXYK repeats have been identified in the human nebulin mRNA (M1 to M185); additional repeats were identified in the human and murine genomic sequences [16;17]. The N-terminal modules of nebulin (M1-M8) contain binding sites for the thin filament pointed-end capping protein tropomodulin, and modules M163 through M185 are located in and near the Z-disk. The centrally located modules, M9 to M162, are each thought to represent individual actin-binding motifs, and are organized into seven-module super-repeats that match the repeat of the actin filament (see figure 1). This precise arrangement is thought to allow each nebulin module to interact with a single actin monomer and each nebulin super-repeat to associate with a single Tm/Tn complex [18;19].

Nebulin's large size has greatly hindered the identification of NM-causative mutations in the nebulin gene. Although to date many of the human *NEB* mutations are predicted to introduce nonsense codons or frame shifts [20], there are no proven "nebulin null" patients, and this situation may in fact be a lethal condition in humans. Instead, virtually all NM patients appear to produce reduced levels of a truncated nebulin, presumably due to an extensive and complex pattern of alternative splicing [5;21]. We studied four NM patients with a nebulin mutation: Three patients harbored a complete deletion of nebulin exon 55 on both alleles and the fourth patient had a heterozygous single base-pair deletion in exon 45 with an unidentified mutation on the second allele. Exon 55 codes for 35 amino acids that are part of modules M69 and M70 of the ninth super-repeat (figure 1). This in-frame deletion of exon 55, causing a deletion of ~4 kDa at the protein level (which is far below the detection limit of proteins in the (near) mega Dalton weight range), likely causes a mismatch between nebulin and its actin binding sites, thereby reducing binding between nebulin and the thin filament, which might increase nebulin's vulnerability to proteolysis [12]. The single mutation identified in the fourth patient causes a frameshift in exon 45 resulting in a premature stop codon, predicted to lead to the production of a significantly shortened protein with decreased function. Indeed, in line with previous work, our gel electrophoresis studies on skeletal muscle from nebulin-based NM patients indicates that the mutations studied here result in nebulin protein levels that were only ~20% of controls (figure 2).

Protein analysis of the thin filament regulatory proteins revealed significantly reduced actin levels in NM muscle (to 78% of controls, figure 2) which is in line with the reduced thin filament length in NM muscle fibers, as suggested by the confocal microscopy studies with phalloidin (see figure 3 and Ottenheijm et al. [9]). Protein levels of the other major components of the thin filament were, relative to actin, present at (close to) the normal levels found in controls (figure 2B), with the exception that nebulin levels were significantly reduced. These findings suggest that absence of nebulin does not inhibit binding of tropomyosin and the troponin complex to the actin filament. Thus, the reduced nebulin levels in muscle fibers from NEM2 patients result in shorter thin filaments, apparently without major effects on the stoichiometry of other thin filament proteins.

Cross bridge cycling kinetics in nebulin-deficient muscle from NM patients—

A hallmark feature of NM is muscle weakness, which greatly impairs the quality of life of

these patients [3]. Although NM is characterized at the muscle structure level by pathological Z-disks, culminating in the formation of nemaline rods, the number of these rods does not correlate with the severity of muscle weakness observed in these patients [22;23]. This suggests that myofibrillar disarray and rod formation are a secondary phenomenon and are not the main contributors to the development of muscle weakness in NM.

Novel insights into the pathogenesis of NM-associated muscle weakness were obtained recently by our lab. These results indicated that, in agreement with the proposed role of nebulin in maintaining thin filament length, myofibrils from patients with nebulin-based NM contain thin filaments that are shorter and non-uniform in length [9]. The concomitant reduction in thin-thick filament overlap, at a given sarcomere length, was shown to partly explain the force deficit observed in the muscle fibers from these patients. The data presented in the current study provide evidence for the notion that, in addition to dysregulation of thin filament length, altered cross bridge cycling kinetics contribute to muscle weakness in patients with nebulin-based NM.

In skeletal muscle, thick and thin filaments are organized into symmetric arrays that interdigitate and slide past each other as the muscle contracts. This muscle contraction is driven by the cyclic interaction between the myosin-based cross bridges and actin. During this cross bridge cycle, unbound non-force generating cross bridges move to an actin-bound force generating state followed by ATP-driven cross-bridge release back to the non-force generating state [24;25]. Thus, the force a muscle can generate is proportional to the force generated per cross-bridge as well as to the fraction of cross-bridges that generate force. Whether the fraction of force generating cross bridges is different between NM and control muscle fibers can be evaluated from ktr and tension cost measurements. For such evaluation, we used the analytical framework proposed by Brenner and co-workers [15] in which the transition between the weakly and strongly bound cross bridges was described by two apparent rate constants; one for cross bridge attachment (f_{app}) and one for cross bridge detachment (g_{app}). In this model the tension cost (ATP consumption rate normalized to tension and fiber volume) is directly proportional to the detachment rate (g_{app}) of myosin cross bridges from actin. Thus, the increased tension cost in NM fibers (figure 5B) indicates that the detachment rate is increased in NM fibers. In this framework, the rate constant of force redevelopment (Ktr) is proportional to $f_{app} + g_{app}$, and the fraction of cross bridges attached to actin, to $f_{app}/(f_{app} + g_{app})$. Thus, the decrease in Ktr of NM fibers, together with the notion that g_{app} is increased, indicates that f_{app} must be reduced and that the reduction must be larger than the increase in g_{app}. Combined, this leads to the conclusion that the fraction of force generating cross bridges is reduced in NM fibers, contributing to the force deficit observed in muscle fibers from these patients. It should be noted that in addition to altered cross bridge cycling kinetics, the fast-to-slow fiber type switch in NM muscle (figure 2C) might also contribute to the observed muscle weakness in these patients (fast fibers from the control subjects showed a trend towards higher force production when compared to slow fibers, 88 ± 5 vs. 71 ± 8 mN/mm^2, respectively.).

Reduced calcium sensitivity in nebulin-deficient muscle from NM patients—*In vivo*, skeletal muscle typically does not perform maximum isometric contractions, but shortens during submaximal activation. Thus, submaximal parameters of muscle function provide relevant physiological information. To test whether submaximal force generation is affected in nebulin-based NM, we exposed permeabilized muscle fibers to various calcium concentrations and determined ensuing force level. As shown in figure 4, we found significantly reduced calcium sensitivity of force generation in the nebulin-deficient fibers from NM patients, suggesting that in addition to maximal force generation, the capacity for submaximal force generation is greatly impaired.

The molecular mechanism(s) underlying the changes in cross bridge cycling kinetics and calcium sensitivity in NM muscle are unknown. We found that the biopsies from the tested NM patients contained mainly fibers expressing slow MHC isoforms, which are known to exhibit slow cross bridge cycling kinetics, whereas the control biopsies contained, in addition to slow isoforms, also the faster 2A and 2X MHC isoforms (figure 2C). However, as the NM fibers were compared to control fibers that exclusively expressed slow MHC isoforms, it is unlikely that differences in MHC isoform composition play a role in the observed changes in cross bridge cycling kinetics.

In addition to MHC isoforms, regulatory protein composition has been shown to impact cross bridge cycling kinetics as well as the calcium sensitivity of force generation. However, with the exception of nebulin, NM muscle showed no major changes in total protein content of the regulatory proteins (i.e the troponin complex and tropomyosin). Although troponin isoform expression was shifted towards expression of predominantly slow isoforms, this reflects the shift towards slow MHC isoforms in NM muscle, and is unlikely to account for the observed changes in contractile performance, as the NM data were compared to slow-type control fibers.

It could be speculated that the changes in contractile performance in the NM fibers are a direct effect of nebulin-deficiency. For instance, nebulin's structure and protein binding properties make it well suited to influence the calcium sensitivity of force generation. Nebulin contains ~200 domains of ~35 amino acids that are characterized by the actin binding sequence SDXXYK; these domains make up seven domain super repeats characterized by the Tm/Tn binding motif, WLKGIGW [26]. Biochemical studies have shown that a single nebulin module interacts with a single actin monomer and that each nebulin super repeat interacts with a Tm–Tn complex of the thin filament [27]. The Tm-Tn complex regulates skeletal muscle contraction by a steric blocking mechanism in which in the relaxed state Tm blocks actin's binding site for myosin, and the binding of Ca^{2+} to Tn induces a movement by Tm away from this blocked position [28]. Experimental evidence for the notion that nebulin is involved in regulating the calcium sensitivity of force generation was provided by recent work revealing that the calcium sensitivity of force generation is reduced in nebulin-deficient murine skeletal muscle [10]: similar findings as reported in the present study on nebulin-deficient NM fibers. In addition, studies on murine skleletal muscle revealed that in the absence of nebulin, cross bridge cycling kinetics is altered to reduce the fraction of force generating cross bridges and reduce active force generation [10;11]. It was speculated that the mechanism by which nebulin affects cross bridge cycling might involve nebulin's assocation with actin's N-terminus in subdomain 1 [29], where the myosin cross bridge also binds. Thus, although the mechanisms underlying the altered cross bridge cycling kinetics and the reduced calcium sensitivity of force generation in skeletal muscle from the nebulin-based NM patients require further study, the present work in combination with previous work on nebulin KO mouse models suggest an effect of nebulin-deficiency on contractile performance.

Clinical relevance—The present study suggests that the muscle weakness observed in patients with nebulin-based NM is likely to involve, in addition to dysregulation of thin filament length [9], changes in cross bridge cycling kinetics and a reduction of the calcium sensitivity of force generation (for a schematic, see figure 7). Although the mechanisms underlying these changes in contractile performance are yet to be identified, nebulin-deficiency is likely to play a role. Considering that mutations in the nebulin gene, which typically cause nebulin-deficiency, are the main cause of NM, these findings provide important novel insights into the pathogenesis of NM-associated muscle weakness, and provide a scientific basis for therapeutics aimed at restoring contractile performance of skeletal muscle in NM patients.

Acknowledgments

Thanks to Danielle Pier and Hal Schneider for nebulin gene mutation detection and for Eric Rogers for gel and Western blot analysis. Special thanks to all the patients, their family members, and referring physicians and health care providers, particularly genetic counselor Joanne Taylor, MS CGC, without whom this study would not have been possible. This work was supported by a VENI grant from the Dutch Organization for Scientific Research to C.A.C.O, NIH RO1 AR053897 to H.G., NIH R01 AR044345, MDA3971 from the Muscular Dystrophy Association (USA), the Lee and Penny Anderson Family Foundation, and the Joshua Frase Foundation to A.H.B. DNA sequencing was performed in the MRDDRC Molecular Genetics Core Facility at Children's Hospital Boston supported by NIH-P30-HD18655.

Reference List

1. Wallgren-Pettersson C. Congenital nemaline myopathy: a longitudinal study. Commentationes Physico-Mathematicae 1990;111:1–102.
2. Morris EP, Nneji G, Squire JM. The three-dimensional structure of the nemaline rod Z-band. J Cell Biol 1990;111:2961–2978. [PubMed: 2269662]
3. North KN, Laing NG, Wallgren-Pettersson C. Nemaline myopathy: current concepts. The ENMC International Consortium and Nemaline Myopathy. J Med Genet 1997;34:705–713. [PubMed: 9321754]
4. Sanoudou D, Beggs AH. Clinical and genetic heterogeneity in nemaline myopathy--a disease of skeletal muscle thin filaments. Trends Mol Med 2001;7:362–368. [PubMed: 11516997]
5. Pelin K, Hilpela P, Donner K, Sewry C, Akkari PA, Wilton SD, Wattanasirichaigoon D, Bang ML, Centner T, Hanefeld F, Odent S, Fardeau M, Urtizberea JA, Muntoni F, Dubowitz V, Beggs AH, Laing NG, Labeit S, de la CA, Wallgren-Pettersson C. Mutations in the nebulin gene associated with autosomal recessive nemaline myopathy. Proc Natl Acad Sci USA 1999;96:2305–2310. [PubMed: 10051637]
6. Wang K, Wright J. Architecture of the sarcomere matrix of skeletal muscle: immunoelectron microscopic evidence that suggests a set of parallel inextensible nebulin filaments anchored at the Z line. J Cell Biol 1988;107:2199–2212. [PubMed: 3058720]
7. Witt CC, Burkart C, Labeit D, McNabb M, Wu Y, Granzier H, Labeit S. Nebulin regulates thin filament length, contractility, and Z-disk structure in vivo. EMBO J 2006;25:3843–3855. [PubMed: 16902413]
8. Bang ML, Li X, Littlefield R, Bremner S, Thor A, Knowlton KU, Lieber RL, Chen J. Nebulin-deficient mice exhibit shorter thin filament lengths and reduced contractile function in skeletal muscle. J Cell Biol 2006;173:905–916. [PubMed: 16769824]
9. Ottenheijm CA, Witt CC, Stienen GJ, Labeit S, Beggs AH, Granzier H. Thin filament length dysregulation contributes to muscle weakness in nemaline myopathy patients with nebulin deficiency. Hum Mol Genet 2009;18:2359–2369. [PubMed: 19346529]
10. Chandra M, Mamidi R, Ford S, Hidalgo C, Witt C, Ottenheijm C, Labeit S, Granzier HL. Nebulin alters crossbridge cycling kinetics and increases thin filament activation- a novel mechanism for increasing tension and reducing tension cost. J Biol Chem. 2009
11. Bang ML, Caremani M, Brunello E, Littlefield R, Lieber RL, Chen J, Lombardi V, Linari M. Nebulin plays a direct role in promoting strong actin-myosin interactions. FASEB J. 2009
12. Anderson SL, Ekstein J, Donnelly MC, Keefe EM, Toto NR, LeVoci LA, Rubin BY. Nemaline myopathy in the Ashkenazi Jewish population is caused by a deletion in the nebulin gene. Hum Genet 2004;115:185–190. [PubMed: 15221447]
13. Lehtokari VL, Greenleaf RS, Dechene ET, Kellinsalmi M, Pelin K, Laing NG, Beggs AH, Wallgren-Pettersson C. The exon 55 deletion in the nebulin gene - One single founder mutation with world-wide occurrence. Neuromuscul Disord 2009;19:179–181. [PubMed: 19232495]
14. Stienen GJ, Kiers JL, Bottinelli R, Reggiani C. Myofibrillar ATPase activity in skinned human skeletal muscle fibres: fibre type and temperature dependence. J Physiol 1996;493 (Pt 2):299–307. [PubMed: 8782097]
15. Brenner B, Eisenberg E. Rate of force generation in muscle: correlation with actomyosin ATPase activity in solution. Proc Natl Acad Sci USA 1986;83:3542–3546. [PubMed: 2939452]

16. Donner K, Sandbacka M, Lehtokari VL, Wallgren-Pettersson C, Pelin K. Complete genomic structure of the human nebulin gene and identification of alternatively spliced transcripts. Eur J Hum Genet 2004;12:744–751. [PubMed: 15266303]

17. Kazmierski ST, Antin PB, Witt CC, Huebner N, McElhinny AS, Labeit S, Gregorio CC. The complete mouse nebulin gene sequence and the identification of cardiac nebulin. J Mol Biol 2003;328:835–846. [PubMed: 12729758]

18. Labeit S, Gibson T, Lakey A, Leonard K, Zeviani M, Knight P, Wardale J, Trinick J. Evidence that nebulin is a protein-ruler in muscle thin filaments. FEBS Lett 1991;282:313–316. [PubMed: 2037050]

19. Labeit S, Kolmerer B. The complete primary structure of human nebulin and its correlation to muscle structure. J Mol Biol 1995;248:308–315. [PubMed: 7739042]

20. Lehtokari VL, Pelin K, Sandbacka M, Ranta S, Donner K, Muntoni F, Sewry C, Angelini C, Bushby K, Van den BP, Iannaccone S, Laing NG, Wallgren-Pettersson C. Identification of 45 novel mutations in the nebulin gene associated with autosomal recessive nemaline myopathy. Hum Mutat 2006;27:946–956. [PubMed: 16917880]

21. Sewry CA, Brown SC, Pelin K, Jungbluth H, Wallgren-Pettersson C, Labeit S, Manzur A, Muntoni F. Abnormalities in the expression of nebulin in chromosome-2 linked nemaline myopathy. Neuromuscul Disord 2001;11:146–153. [PubMed: 11257470]

22. Shimomura C, Nonaka I. Nemaline myopathy: comparative muscle histochemistry in the severe neonatal, moderate congenital, and adult-onset forms. Pediatr Neurol 1989;5:25–31. [PubMed: 2712935]

23. Ryan MM, Ilkovski B, Strickland CD, Schnell C, Sanoudou D, Midgett C, Houston R, Muirhead D, Dennett X, Shield LK, De Girolami U, Iannaccone ST, Laing NG, North KN, Beggs AH. Clinical course correlates poorly with muscle pathology in nemaline myopathy. Neurology 2003;60:665–673. [PubMed: 12601110]

24. Huxley AF, Simmons RM. Proposed mechanism of force generation in striated muscle. Nature 1971;233:533–538. [PubMed: 4939977]

25. Lymn RW, Taylor EW. Mechanism of adenosine triphosphate hydrolysis by actomyosin. Biochemistry 1971;10:4617–4624. [PubMed: 4258719]

26. McElhinny AS, Kazmierski ST, Labeit S, Gregorio CC. Nebulin: the nebulous, multifunctional giant of striated muscle. Trends Cardiovasc Med 2003;13:195–201. [PubMed: 12837582]

27. Ogut O, Hossain MM, Jin JP. Interactions between nebulin-like motifs and thin filament regulatory proteins. J Biol Chem 2003;278:3089–3097. [PubMed: 12446728]

28. Gordon AM, Homsher E, Regnier M. Regulation of contraction in striated muscle. Physiol Rev 2000;80:853–924. [PubMed: 10747208]

29. Root DD, Wang K. Calmodulin-sensitive interaction of human nebulin fragments with actin and myosin. Biochemistry 1994;33:12581–12591. [PubMed: 7918483]

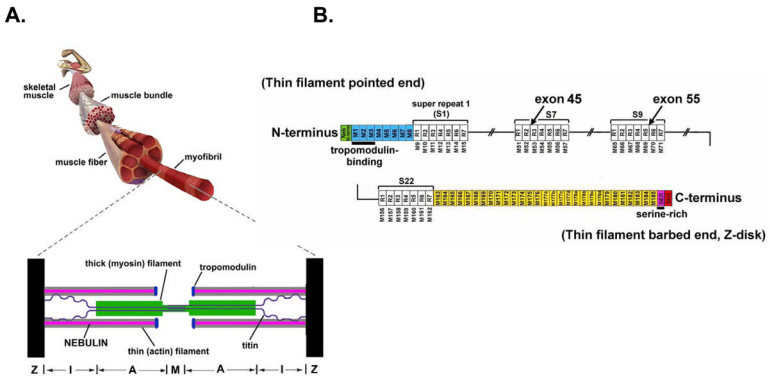

Figure 1.

A) Schematic of a structural organization of skeletal muscle and sarcomere (bottom). B) Schematic of the human nebulin sequence. Nebulin has a highly modular structure, with in the central region (M9–M162) seven modular repeats arranged into twenty-two super-repeats. The four NEM2 patients studied here harbor mutations in exon 45 (one patient) that is part of super-repeat 7, and exon 55 (three patients) that is part of super-repeat 9.

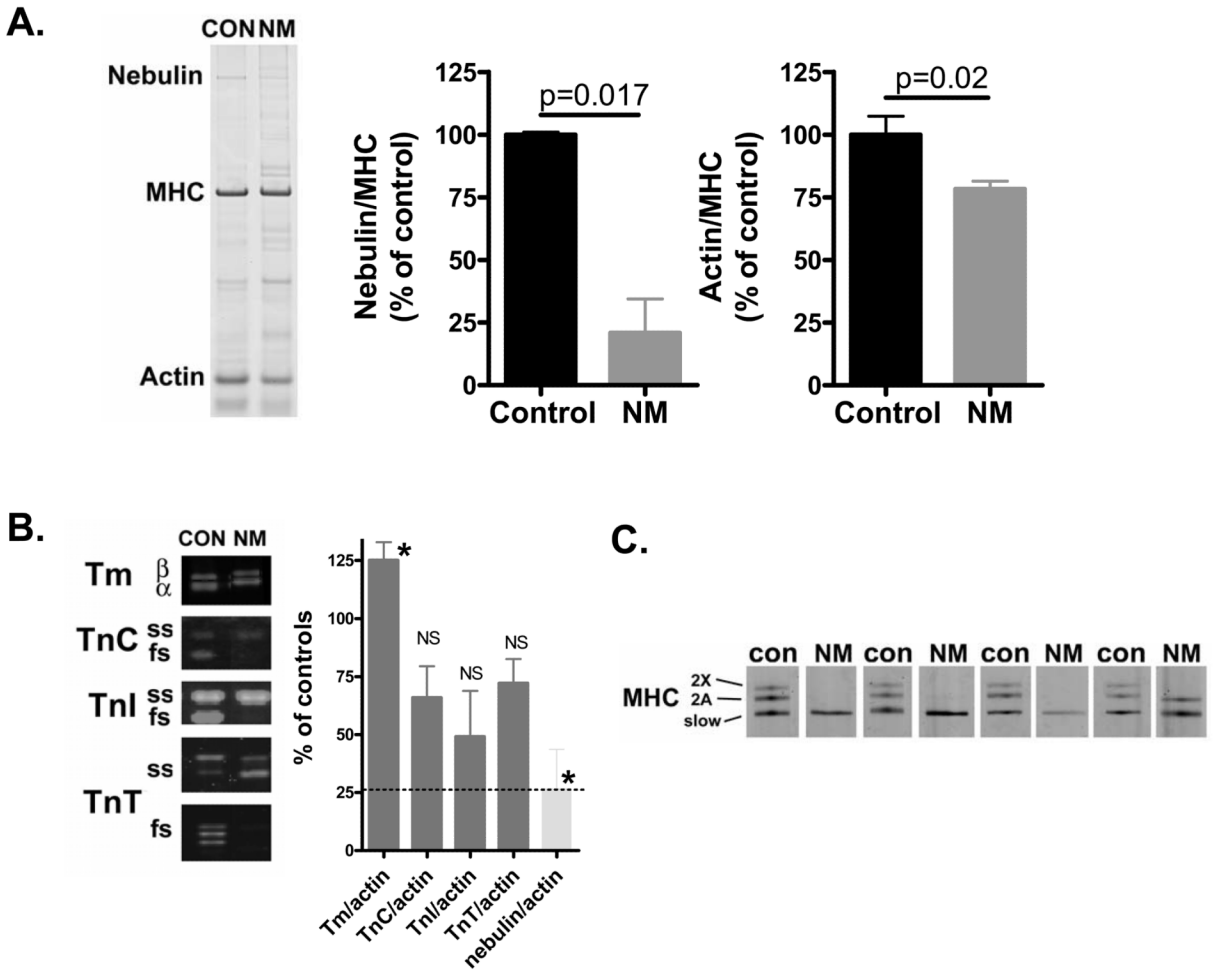

Figure 2.

A) SDS-PAGE (for typical example gel result of a control and NM patient, see left panel; NM patient ID: 174-1) revealed that nebulin protein levels (normalized to MHC) in nebulin-based NM muscle are reduced to ~20% of the nebulin levels found in control muscle (middle panel). Actin protein levels in nebulin-based NM muscle are reduced to ~80% of controls (right panel). B) Expression analysis of proteins regulating sarcomeric force generation (left panel shows Western blot result for a control and NM patient; NM patient ID: 4–5). Total protein levels of tropomyosin, relative to actin, were slightly increased in NM. Total protein levels of troponin C, I, and T, relative to actin, were on average reduced but this reduction was not statistically significant. In light grey bar the nebulin/actin ratio is shown, illustrating the predominant decrease in nebulin protein level. Note that NM muscle showed a shift towards slow isoforms of the troponins (see text for details). C) Specialized SDS-PAGE to separate MHC isoforms in muscle from the four NM patients and four control subjects. Note the strong predominance of myosin heavy chain slow in NM muscle, whereas control muscle expresses slow, 2A, and 2X isoforms. NM patient IDs, from left to right: 76-1, 4-5, 4-4, 174-1.

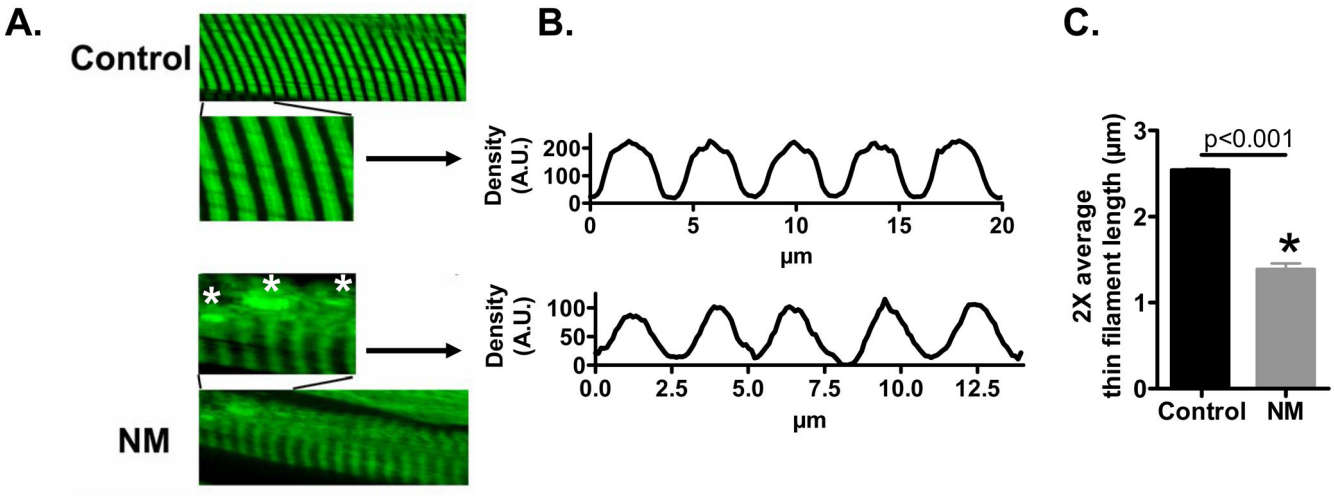

Figure 3.

Myofibrils from controls and nebulin-based NM patients stained for actin. A) Actin staining with phalloidin shows broad and homogenous staining in control myofibrils, whereas actin staining intensity in NM myofibrils gradually decreases from Z-disk towards the middle of the sarcomere. Analysis of phalloidin line scan intensities (B) revealed significantly reduced average thin filament (TF) lengths in NM myofibrils (C).

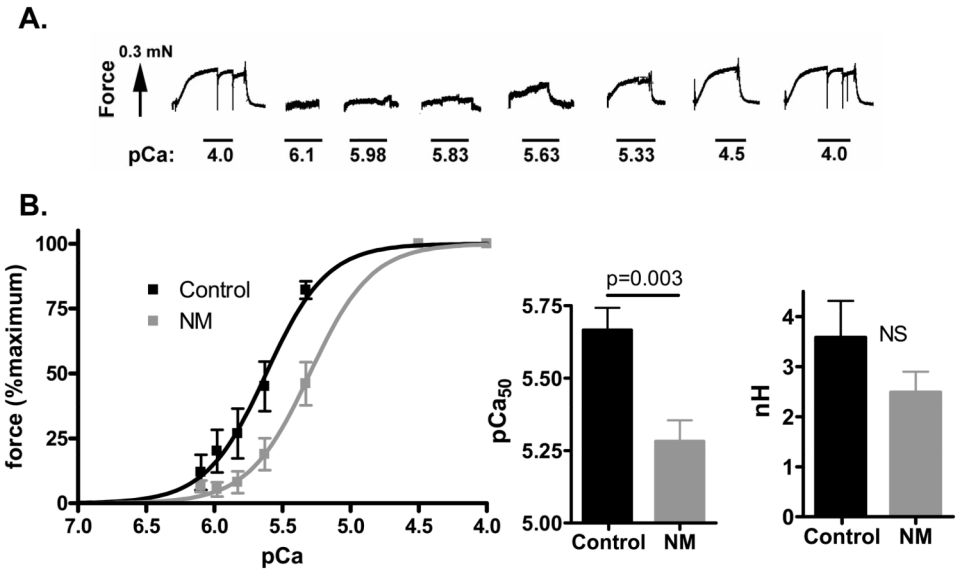

Figure 4.

Force–Ca^{2+} characteristics of skinned muscle from NM and control muscle (note that the results from NM muscle fibers were compared to those from control muscle fibers expressing solely MHC slow). A) Typical chart recording showing the force response to incremental Ca^{2+} concentrations in a NM (174-1) fiber preparation B) Left panel: the force generated in response to incubation with incremental increase of [Ca^{2+}]; note the rightward shift of the force–Ca^{2+} relationship in NM vs control muscle. Middle panel, the Ca^{2+} concentration needed for 50% of maximal force generation was significantly higher (i.e., lower pCa_{50}) in NM vs control muscle, whereas no difference was found in the Hill coefficient (nH, right panel).

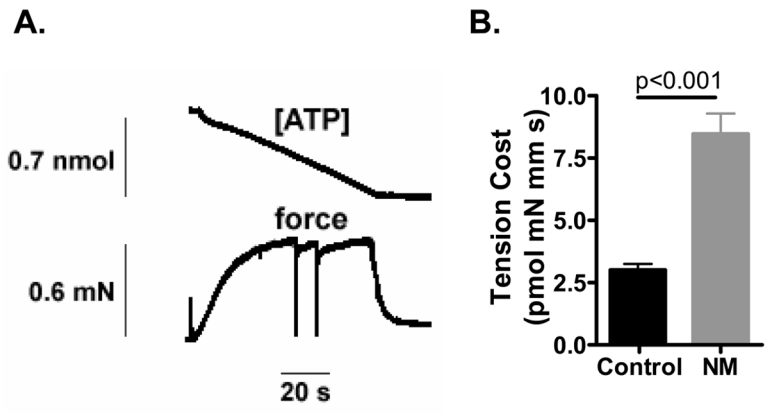

Figure 5.

Tension cost of NM and control fibers. A) Example of a maximally activated NM (174-1) fiber bundle (pCa 4.5) with developed force at bottom and [ATP] at the top. The slope of the [ATP] vs time trace was divided by fiber volume (in mm^3) to determine ATP consumption rate. B) ATP consumption rate was normalized to tension to determine the tension cost. Tension cost is significantly higher in NM fibers.

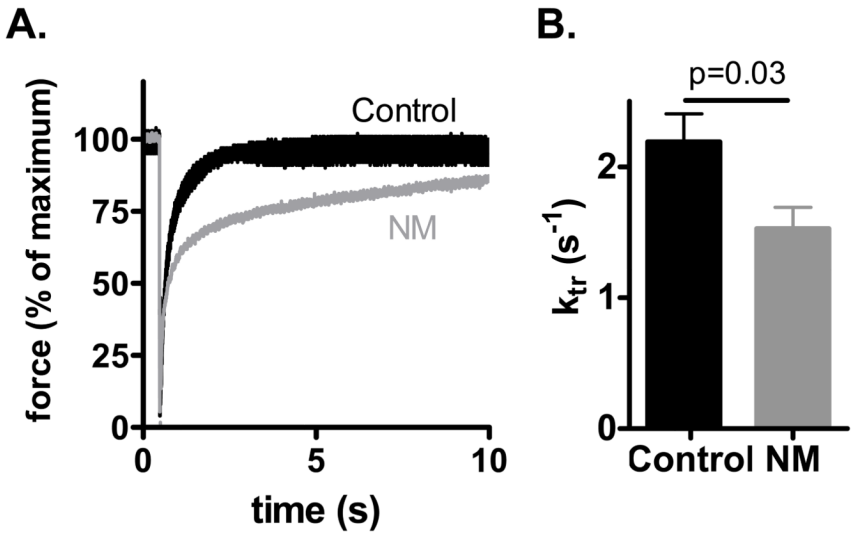

Figure 6.

K_{tr} measurements of NM and control fibers. A) Example of k_{tr} measurement at pCa 4.5 with superimposed the results of a NM (174-1) and a control fiber. B) K_{tr} is significantly lower in NM compared to control fibers.

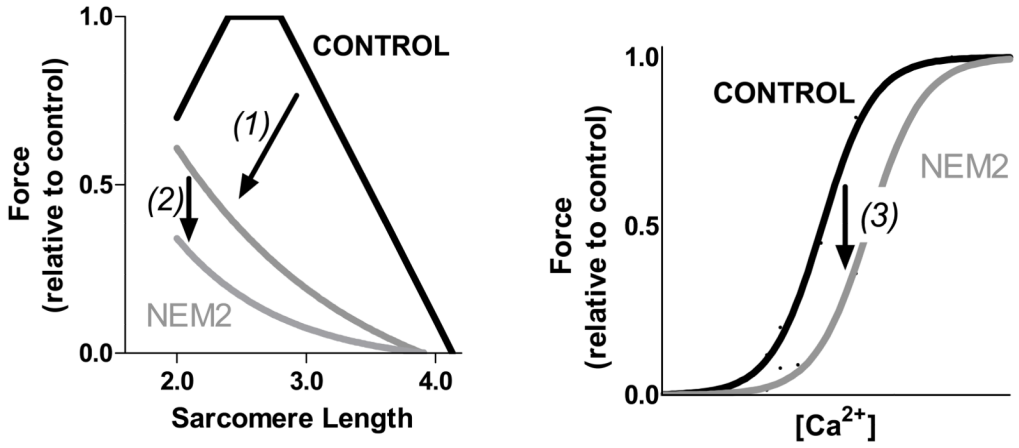

Figure 7.

Schematic of the mechanisms underlying muscle weakness in NEM2 patients. In NEM2 patients, force is depressed by *(1)* decreased and non-uniform thin filament lengths to reduce the amount on thin-thick filament overlap in a sarcomere length dependent manner (for details see Ottenheijm et al. [9]); *(2)* altered cross bridge cycling kinetics to reduce the fraction of force generating cross bridges; *(3)* a decrease of myofilament calcium sensitivity to reduce submaximal force generation.

Table 1

Clinical and pathological characteristics of nemaline myopathy patients and characteristics of control subjects.

Patent ID[a]	Biopsy ID	NEB mutation[b]	Gender	Biopsy location	Age at biopsy	Fiber typing	Rod characteristics	Clinical form[d]	Age of onset	Maximal motor ability	Clinical Status
4-4	T11	Homozygous *NEB* del e55 c.7431+1916_7536+372del p.Arg2478_Asp2512del	M	Rectus abdominus	4 mo	Extreme type 1 predominance	Rods primarily located in subarcolemmal region of most fibers, originating from Z-bands	Severe	Birth	Never walked	Died at 19y; Never walked; Required mechanical ventilation and G- tube from infancy
4-5	T12	Homozygous *NEB* del e55 c.7431+1916_7536+372del p.Arg2478_Asp2512del	M	Abdominal wall	2 mo	Extreme type 1 predominance and atrophy/hypotrophy	Rods primarily located in subarcolemmal region of almost all type 1 fibers, especially around nucleus and occasionally along Z-bands	Severe	Birth	Never walked	Alive at 21y and has required G-tube and mechanical ventilation since infancy; Never sat or walked
76-1	T46	c.[5722delA] + [?][c] p.Ser1908AlafsX8	M	Quadriceps	2 y 5	Extreme type 1 predominance and minimal fibre size variation	Abundant sarcoplasmic rods within subsarcoplasm and between muscle fibrils	Typical	Birth	Walked at 2y	Died at 15 y; Walked independently from 2 y until death and required nocturnal Bi-pap by 9 y.
174-1	T124	Homozygous *NEB* del e55 c.7431+1916_7536+372del p.Arg2478_Asp2512del	F	Quadriceps	7 mo	Type 1 predominance and hypotrophy, with moderate fiber size variation.	Rods in numerous fibers	Intermediate	Birth	Walked with walker at ~2.5y	Alive at 9y. Requires mechanical ventilation 16 hours per day, G-tube and oral feeds, and wheelchair for longer distances
NA	-	Unaffected	F	Quadriceps	30y	-	-	-	-	Normal	-
NA	-	Unaffected	M	Quadriceps	45	-	-	-	-	Normal	-
NA	-	Unaffected	M	Quadriceps	32	-	-	-	-	Normal	-
NA	-	Unaffected	M	Quadriceps	45	-	-	-	-	Normal	-

[a] Patients 4-4, 4-5 and 174-1 were previously described by Lehtokari et al. 2009 as Patients 2-1, 2-2 and 5, respectively. Patients 4-4 and 4-5 were also included in the original study by Anderson et al. (2004).

[b] Numbering is based on current standard numbering scheme, starting from the initiating ATG for cDNA numbering, and with the first methionine for amino acid numbering. Reference sequences were the NCBI accession numbers: cDNA, NM_001164507.1; protein, NP_001157979.1.

[c] This mutation results in g.[75887delA] on genomic reference sequence NG_009382.1. As indicated by "+ [?]", the second mutation in this patient has not yet been identified.

[d] Clinical form of NM as defined in Sanoudou and Beggs (2001).